

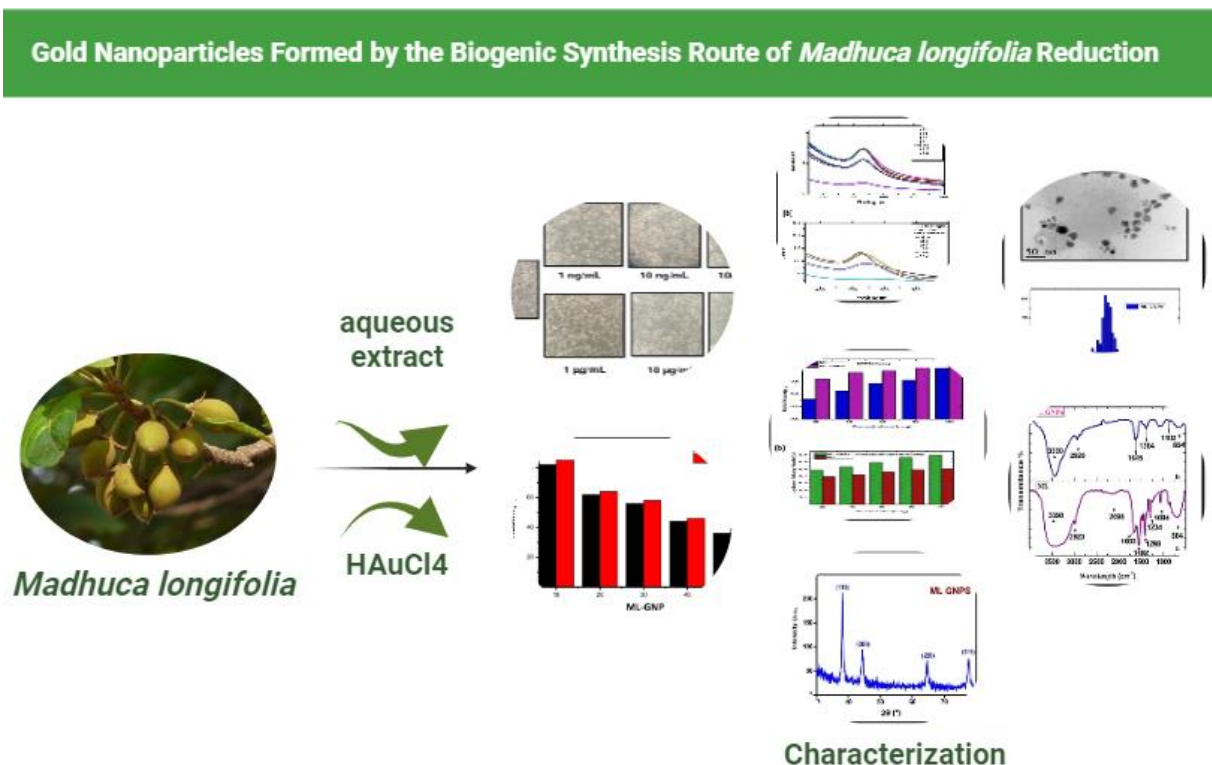
Evaluating the Therapeutic Importance of Gold Nanoparticles Formed by the Biogenic Synthesis Route of *Madhuca longifolia* Reduction

Manikandan Dhayalan,^a Sheikdawood Parveen,^b Sathiyapriya Thirumalaisamy,^c Faruq Mohammad,^d Hamad A. Al-Lohedan,^d Savaas Umar Mohammed Riyaz,^e Rakshi Anuja Dinesh,^f Jayant Giri,^g Antony Stalin,^h Gangireddy Rajasekhar Reddy,ⁱ Natarajan Anandakumar,^j and Saurav Mallik^k

* Corresponding authors: manikandandhayalan88@gmail.com; jayantpgiri@gmail.com

DOI: 10.15376/biores.19.1.823-841

GRAPHICAL ABSTRACT



Evaluating the Therapeutic Importance of Gold Nanoparticles Formed by the Biogenic Synthesis Route of *Madhuca longifolia* Reduction

Manikandan Dhayalan,^a Sheikdawood Parveen,^b Sathiyapriya Thirumalaisamy,^c Faruq Mohammad,^d Hamad A. Al-Lohedan,^d Savaas Umar Mohammed Riyaz,^e Rakshi Anuja Dinesh,^f Jayant Giri,^g Antony Stalin,^h Gangireddy Rajasekhar Reddy,ⁱ Natarajan Anandakumar,^j and Saurav Mallik^k

Herbal plants have been used, in light of their responsiveness and wide availability, for the construction of a pioneering nanomaterial. In this study, a colloidal suspension of gold nanoparticles (GNPs) was synthesized from an extract of *Madhuca longifolia* (ML) using chloroauric acid. For biomedical applications, *Madhuca longifolia* (ML) was used as a bioreductant as well as a capping agent. The formed ML-GNPs were analyzed using different analytical techniques, antioxidant assays, and thiazolyl blue formazan assay against A549 cell lines to evaluate clinical relevance. They were further evaluated for their influence on antimicrobial activity using a disc diffusion test against two different microorganisms, *Proteus vulgaris* and *Micrococcus luteus*. The ML-GNPs produced had good antioxidant, antibacterial, and anticancer activities. The conformation of the XRD spectra with prominent characteristic planes was indexed to the face-centered cubic (fcc)-structured GNPs. Surface morphology analysis was used to determine the particle size of the GNPs. Fourier transform infrared spectra of the samples were used to determine the analogs for strong H bonding. The MIC values of biogenic GNPs against both strains of *Proteus vulgaris* and *Micrococcus luteus* was calculated as 0.29 and 0.96 g/mL, respectively, and triclosan was considered as 0.4 and 2 g/mL, respectively. The findings of this study will be beneficial for future studies of the therapeutic potential of ML-GNPs. Actively, ML-GNPs can be a capable material for formulating nanomedicines after subsequent clinical experiments.

DOI: 10.15376/biores.19.1.823-841

Keywords: Green synthesis; Gold nanoparticles; Seed extract; *Madhuca longifolia*; MTT assay

Contact information: a: Department of Prosthodontics, Saveetha Dental College & Hospitals, Saveetha Institute of Medical and Technical Sciences (Saveetha University) Chennai - 600 077, Tamil Nadu, India; b: Bio Inspired Material Research Laboratory, Dr. Mahalingam College of Engineering and Technology, Pollachi-642002, Tamil Nadu; c: Department of Chemistry, Coimbatore Marine College, Coimbatore-641032, India; d: Department of Chemistry, College of Science, King Saud University, P.O. Box 2455, Riyadh 11451, Saudi Arabia; e: PG & Research Department of Biotechnology Islamiah College (Autonomous), Vaniyambadi - 635752, Tamil Nadu, India; f: Faculty of Science, School of Chemistry and Molecular Biosciences, The University of Queensland, St. Lucia, Brisbane, Queensland, Australia; g: Department of Mechanical Engineering, Yeshwantrao Chavan College of Engineering, Nagpur, Maharashtra, India; h: Institute of Fundamental and Frontier Sciences, University of Electronic Science and Technology of China, Chengdu, 610054 China; i: NACL Industries Limited, R&D Center, Hyderabad, RR District - 509228, Telangana, India; j: Department of Education, The Gandhigram Rural Institute, Gandhigram, Dindigul-624302, India; k: Department of Environmental Health, Harvard T H Chan School of Public Health, Boston, MA, USA;

* Corresponding authors: manikandandhayalan88@gmail.com; jayantpgiri@gmail.com

INTRODUCTION

Nanotechnology focuses on the concentration and formation of nanoparticles (NPs) through wide variations in their shape, size, and chemical composition. Numerous therapeutic and commercial uses have been developed because of the unique features of NPs. Metal nanoparticles are well known and have attracted attention because of their optical characteristics. Gold nanoparticles (GNPs) are the most widely investigated nanostructures for biological applications (Kucherenko *et al.* 2019). GNPs offer a distinctive viewpoint through enabling the nanoscale miniaturization of electrochemical sensors. The size of GNPs, which have a gold core and gold surface coating, can range from a few to several hundred nanometers. GNPs have made major contributions to the field of biomedical applications because of their interesting and distinctive physicochemical features.

GNPs can be formed using various physical, chemical, and biological methods (Khan *et al.* 2014; Sengani *et al.* 2017; Jayashree *et al.* 2022). GNPs can be produced by chemical degradation (Shameli *et al.* 2010), electrochemically (Yin *et al.* 2003), X-ray irradiation (Darroudi *et al.* 2013), ultra-radiation treatment (Darroudi *et al.* 2011a), photochemical reduction (Kutsenko and Granchak 2009), ultrasonic aid (Darroudi *et al.* 2012), microwave (Kahrilas *et al.* 2014), and laser ablation (Darroudi *et al.* 2011a,b). Although GNPs are biocompatible, the use of toxic substances during the manufacturing process results in poisonous chemicals being adsorbed on their surfaces, severely restricting their use in the medical field (Smitha *et al.* 2009; Panda and Deepa 2011). Because of the use of toxic chemicals and expensive methodologies that result in unwanted byproducts, physical and chemical approaches are destructive and affect the environment and living beings, whereas biological synthesis can be an easy, inexpensive, and environmentally beneficial alternative (Patil and Kim 2017; Dhayalan *et al.* 2021). Plants (Patil *et al.* 2017; Tahir *et al.* 2023; Patil *et al.* 2018), and microbes (Patil *et al.* 2019) are the only two examples of sources that are biological synthesis that act as stabilizing and reducing agents. The use of plant extracts in the biotic synthesis of NPs is unusual because it is simpler, more stable, and has a faster pace of synthesis than other biological media. The reduction of gold chloride to metallic gold can be implemented using a variety of methods, including chemical reduction, electrochemical reduction, and photoreduction. The choice of method will depend on the specific application (Homa *et al.* 2022). The reduction of metallic ions to Au(0) occurs when polyphenolic compounds undergo a keto-enol form transition during the manufacture of GNPs. In kaolin-supported GNPs, kaolin interceded by mentha extract were described as green refractories by Yang *et al.* (2022).

Ahati *et al.* (2022) reported a new chemotherapeutic drug containing GNPs and *Citrus reticulata* seed juice for dealing with carcinoma. The biosynthesized GNPs scavenged DDPH with an IC₅₀ of 87 µg/mL. The prepared nanoparticles were toxic to THP-1 cells (Abdoli *et al.* 2021). Several plant extracts, including coriander, mango, *Gymnocladus assamicus*, *Aloe vera*, *Piper nigrum*, *Eucalyptus globules*, *Sida cordifolia*, *Rosa damascene*, *Pogostemon benghalensis*, olive, *Rosa indica*, *Pistacia integerrima*, *Lippia citriodora*, Sweet scented geranium, and pomegranate, have been extensively studied as reductants for gold salts used in the manufacture of GNPs (Elia *et al.* 2014).

In a comparative analysis of the synthesized nanoparticles, silver nanoparticles (AgNPs) derived from the *Blumea lacera* (*B. lacera*) leaf extract demonstrated notable anticancer and antioxidant activities. Against the human lung carcinoma cell line A549, AgNPs exhibited a minimal inhibition concentration (IC₅₀) of approximately 20 µg/mL,

indicating their potential as eco-friendly anticancer agents. Moreover, AgNPs displayed robust antioxidant properties, with an IC₅₀ value of approximately 6 µg/mL, demonstrating their effectiveness in neutralizing oxidative stress. The synthesized AgNPs, characterized by a sharp surface plasmonic resonance band at 430 nm and spherical morphology with an average particle size of 12.52 nm, present a promising avenue for cancer treatment and antioxidative interventions. (Pandey *et al.* 2023)

On the other hand, palladium nanoparticles (PdNPs) generated through biogenic synthesis using *Madhuca longifolia* leaves (MLE) have demonstrated their own set of activities (Chinky *et al.* 2023). In the biological screening, MLE@PdNPs were tested against human lung cancer cells A549 and various bacterial strains, including *S. aureus*, *K. pneumonia*, *Salmonella*, and *E. coli*. The IC₅₀ value against lung cancer cells A549 was calculated to be 29.2 µg/mL, suggesting its potential biomedical applications. Additionally, MLE@PdNPs exhibited anti-bacterial activity, with IC₅₀ values ranging from 26.0 to 35.2 µg/mL against *S. aureus*, *K. pneumonia*, *Salmonella*, and *E. coli* bacterial strains, indicating their efficacy in combating bacterial infections (Gangwar *et al.* 2023). While both AgNPs from *B. lacera* and PdNPs from MLE show promising anticancer activities, AgNPs excel in antioxidant properties. On the other hand, MLE@PdNPs demonstrated effectiveness against both lung cancer cells and bacterial strains, highlighting their potential for versatile biomedical applications. The choice between the two nanoparticles depends on the specific requirements of the intended application, whether it is cancer treatment, antioxidative interventions, or antibacterial therapy.

Due to the global emphasis on green nanotechnology research, a variety of nanomaterials are now being used in applications that are both medically and environmentally acceptable. Scientists are interested in investigating the green synthesis of GNPs by utilizing plants' secondary metabolites due to a number of advantages over traditional physical and chemical synthesis, including a straightforward, one-step synthesis process, cost-effectiveness, energy efficiency, and biocompatibility (Hosny *et al.* 2022). This study describes an ecologically acceptable approach to produce GNPs using *Madhuca longifolia* extract and gold ion reduction. The biosynthetic process was investigated using ultraviolet (UV) spectroscopy and the crystal structure was resolved using X-ray diffraction (XRD). The biological compounds were analyzed using Fourier transform infrared (FTIR) spectroscopy. The high-resolution transmission electron microscopy (HR-TEM) analysis was used to study the morphology of GNPs generated throughout the biosynthesis process. The antioxidant, antibacterial, and anticancer properties of the ML- and ML-GNPs were also studied.

EXPERIMENTAL

Materials

Glass trial tubes, mugs, conical flasks, gauging jars, petri dish and funnels, were obtained from Airblow Pvt. Ltd., Chennai, Tamilandu.

Chemicals, such as chloroauric acid, dimethyl sulfoxide (DMSO), (DPPH)- CAS Number: 1898-66-4, sulfuric acid, methanol, ascorbic acid, monosodium phosphate (MSP), thiazolyl blue formazan, disodium hydrogen phosphate, ethylene diamine tetra acetic acid, ammonium molybdate, acridine orange, sodium bicarbonate, and NaCl, were all obtained was purchased from SRL, Bombay, India. Cell culture: A549 was obtained from the National Center for Cell, India. The culture media included penicillin,

gentamycin, amphotericin, streptomycin, fetal calf serum, and casein acid hydrolysate. The bacteriological samples *Escherichia coli* and *Staphylococcus aureus* were obtained from Microbial Type Culture Collection and Gene Bank (MTCC), Chandigarh, India (<https://mtccindia.res.in>).

Taxonomy and Collection of Seed Extract

Madhuca longifolia seeds (family *Sapotaceae*) were freshly collected from the arenas of Pollachi and Coimbatore districts, TamilNadu, India. The following active chemical and biological molecules constituents are present in seed extract of *Madhuca longifolia* such as oleanolic acid, madhunolic acid, madhushazone, madhusalmone, 3',4'-dihydroxy-5,2'-dimethoxy-6,7-methylendioxy isoflavone, saponin A&B, D-glucose, L-rhamnose, L-arabinose, D-fructose, triglyceride of palmito-distearin, triglyceride of oleo-stearo-palmitin, nonacosane, and linoleic acid (Roat *et al.* 2023). The seeds were meticulously cleaned, and the cut pieces were stored in sunshine for an entire week. The dried seed pieces were powdered and cooked in water by refluxing for 60 min. The powdered seed powder was stored at -25 °C for further use. Deionized water (100 mL) containing fine seed powder (5 g) was heated for 30 min before cooling and weeding using Whatman filter paper No. 1.

Preparation of Metal Nanoparticles

A consistent amount (1 mL) of produced seed extract were transferred to ten distinct glass tubes, followed by the addition of 1×10^{-4} M chlorauric acid in 0.1 to 0.5 mL increments to various collections. Subsequently, 10 mL of deionized H₂O was added and allowed to complete the reaction. The pH range of 7 to 13 was used to test the chemical stability of GNPs. Based on their characterization, the ideal synthetic condition (pH 7.0 at room temperature) was deduced, and a capacity of 0.4 mL of tumbling agent (Seed - *Madhuca longifolia*) was required to produce nanoparticles by dissolving gold ions.

Characterization of Metal Nanoparticles

An ultraviolet–visible spectroscopy was used to measure the absorbance of ML-GNPs. A UV-1601 spectrophotometer (Shimadzu, Kyoto, Japan) was used to retrieve spectral data from the colloidal gold suspension itinerant from 200 to 1100 nm. The purpose was to pinpoint the functional component that was reduced by gold ions and nanoparticle formation. The IR spectra in the region from 500 to 4000 cm⁻¹ were analyzed for NPs. The XRD technique used to evaluate the crystallite size of synthesized GNPs. HR-TEM was achieved using FEI Tecnai (OR, USA).

Antioxidant Activity

2, 2-Diphenyl-1-picrylhydrazyl (DPPH)

This analysis was performed to assess the capacity of the seed extract to scavenge free radicals (Faramarzi and Hrootanfar 2011). The experimental solutions (10 to 100 g/mL) were cultivated with a freshly prepared solution of DPPH in methyl alcohol (4/1000 w/v) in a series of dilutions. After 30 min of mixing, the reaction was allowed to proceed at room temperature. The absorbance was measured at 516 nm, and a reduction in absorbance was directly correlated with increased DPPH activity for the identification and elimination of free radicals. This technique was done thrice to obtain three values. The vitamin C solvate in purified H₂O served as a benchmark for comparison, with methanol

(95%) serving as the blank. The following formula (Eq. 1) was used to determine the capacity of the sample to neutralize DPPH radicals,

$$[(A_c - A_t) / A_c] \times 100 \quad (1)$$

where A_c is the absorbance of the control, and A_t is the absorbance of the test sample.

Phosphomolybdenum assay

The green phosphomolybdenum complex production technique (Elia *et al.* 2014) was used to assess the antioxidant activity of ML-GNPs. In a 4 mL vial, a larger sample of 100 μ L solution was mixed with 1 mL of a mixture solution (0.6 M H_2SO_4 , 28 mM triphosphate, and 4 mM $(NH_4)_6Mo_7O_{24}$). The vials were then sealed and protected for 90 min in a water bath at 94 $^{\circ}C$, and the absorbance at 695 nm was measured against a blank; afterward, samples were chilled. The reported results are values expressed as % Phosphomolybdenum Reducing Potential (PRP). The percentage of reticence was determined using the Eq. 2,

$$PRP(\%) = (1 - A/A_c) \times 100 \quad (2)$$

where A_c is the absorbance of the control and A_t is the absorbance of the test sample.

Cytotoxicity (MTT) assay

The MTT reduction assay was used to assess cell viability. A549 cells were seeded at a thickness of 5103 cells culture in 96-well plates for 1 d in 200 L of RPMI containing 10% FBS. After removing the cell culture supernatants, numerous doses (0.11 to 100 g/mL) of the examination sample (ML-GNPs) were combined and nurtured for 48 h. Following handling, the cells were cultivated for 4 h at 38 $^{\circ}C$ with MTT (10 L, 5 mg/mL), and at that time they were held for 1 h at chamber temperature with DMSO. To read the plates at 592 nm, a scanning multiwell spectrophotometer (Sunrise TM, TECAN, Männedorf, Switzerland) was used. The information reflected the average of six separate experiments (Oladipo *et al.* 2017):

$$\text{Cell viability (\%)} = \text{Mean OD/Control OD} \times 100 \quad (3)$$

Antimicrobial Activity

Microorganisms, such as *Micrococcus luteus* and *Proteus vulgaris*, were used to determine the antibacterial ability of ML-GNPs using a good diffusion technique. The various compositions of the examination taster used were (25, 50, 75, and 100 μ g/mL) in addition to the shafts of the agar media. Tetracycline is a routinely administered antibiotic. The incubation was completed at 38 $^{\circ}C$ for 48 h. The ZOI was assessed to define antibacterial action after incubation.

Minimal inhibitory concentration (MIC)

Bacterial growth in LB potage was followed for 24 h under aerobic conditions at 38 $^{\circ}C$. A hemocytometer was used to count the cells; in addition a cell interruption (1105 cells/mL) was set. In triplicate microtiter wells, 100 μ L of cell suspension was dispensed, 100 μ L of interruption holding different concentrations of nanoparticles in LB mediocre, and then mixed. Triclosan (Ref), was used to associate the antiseptic potential of GNPs. Dimethyl sulfoxide (DMSO) was used to dissolve triclosan, which was then diluted with sterilized LB medium to provide medication doses ranging from 0.0313 to 1,024 g/mL.

The development of the cells was monitored spectrophotometrically at 600 nm for 24 h at ambient humidity (Powerserve XS Biotech, OR, USA) while they were cultured *via* either NPs or commonly used antibacterial substances. The control consisted of wells containing cells devoid of GNPs. The MIC was resolute as the lowest concentration of GNPs that prevented *Proteus vulgaris* and *Micrococcus luteus* cells from growing by 50% under experimental conditions.

Statistical Analysis

Inhibition percentages compared to those of the control were used to express the findings. The examinations were conducted three times, mean \pm SD is used for the presentation of the data.

RESULTS AND DISCUSSION

Characterization

Ultraviolet–visible spectroscopy analysis

The tube containing the GNPs suspension exhibited a distinctive gold peak and polydispersity (Fig. 1b). Figure 1a illustrates the UV–visible spectrum obtained in the presence of LPBs. The 540 nm peak in the UV–visible captivation band verifies the synthesis of GNPs (Ohadi *et al.* 2018; Abdoli *et al.* 2021). An immersion band range at 528 nm after treating Au³⁺ ions with *Madhuca longifolia* extract was recognized as stable GNP formation. The reaction between the tumbling agent and the predecessor was identified through adjusting the pH and then volume using UV-visible spectroscopy. The concentrations of HAuCl₄ and *M. longifolia* aqueous extract were fixed. The main spectrophotometric indicator of GNP production was the switch from yellow to dark violet. A peak with a high intensity was observed at the maximum of HAuCl₄ at 530 nm at pH 7. The intensity and yield of GNPs decreased as pH increased from 7 to 13, indicating that pH difference may disturb the biogenic synthesis of GNPs. (Fig. 1a). The optimum concentration was fixed using a similar absorbance study. Through the augmentation of the *M. longifolia* extract, the absorbance also increased (Fig. 1b). Based on this finding, the optimal pH and volume of *M. longifolia* extract for the production of GNPs were calculated as 7 and 0.4 mL, respectively.

High resolution transmission electron microscopy (HR-TEM)

A distribution of particle diameters in the range of 10 to 50 nm was judged to be pragmatic for the colloidal GNPs. A spherical, atypical form of the GNPs were produced. Figure 2a depicts GNPs as dispersed particles with small interparticle distances. HRTEM, in conjunction with PSA analysis, has been used for surface morphology study and to determine the particle size of the GNPs. The engineered nanoparticles exhibited a variety of morphologies; most were sphere-shaped and had an average size of 50 nm, which corresponds to the results of the TEM analysis from this study (Fig. 2B) (Faramarzi and Forootanfar 2011). One possible explanation for the different sizes and shapes of NPs is the presence of chemicals in the aqueous extract of *C. behen* leaf, which converts Au ions to NPs (Singh *et al.* 2011).

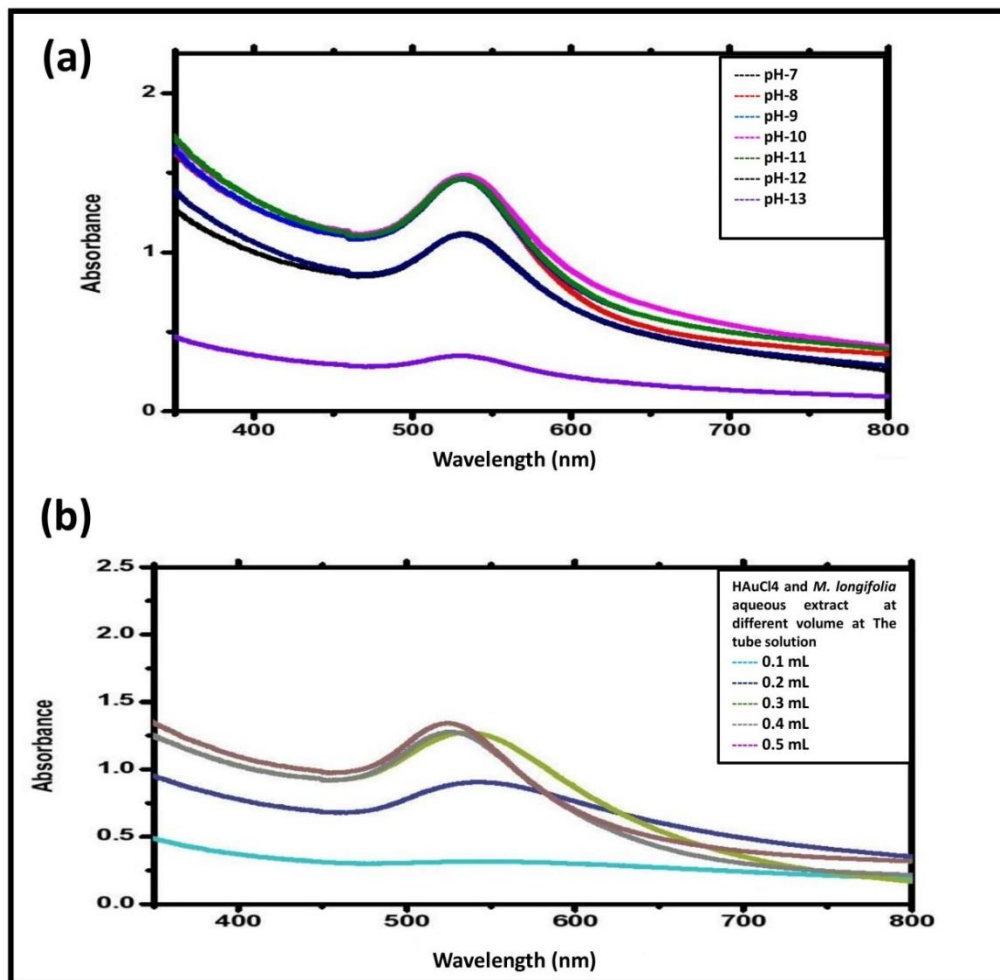


Fig. 1. UV-Visible absorbance graph. The optimal pH and volume of *Madhuca longifolia* extract aimed at the synthesis of GNPs was projected to be 7 and 0.5 mL, respectively (Fig. 1a). The tube sample displayed representative peak of GNPs, respectively, with polydispersity of nanoparticles (Fig. 1b).

Particle size analysis

Typical ML-GNP particle sizes ranged from 10 to 50 nm (Fig. 2b). The GNPs synthesized using the ML-extract were polydisperse, which is a common problem with green synthesis. The particle size scattering is shown in Fig. 2b, with synthesized GNPs having mass average size of 50.00 ± 3.46 nm.

Fourier Transform Infrared (FTIR) Spectroscopy

The surface chemistry of ML-GNPs was investigated using FTIR spectra. *Madhuca longifolia* seed extract (ML) spectral data showed dominant peaks at 3398, 2923, 2098, 1605, 1492, 1298, 1234, and 804 cm^{-1} (Fig. 3a). Peaks observed in the prepared ML-GNPs were at 3390, 2926, 1645, 1364, 1102, and 654 cm^{-1} (Fig. 3b).

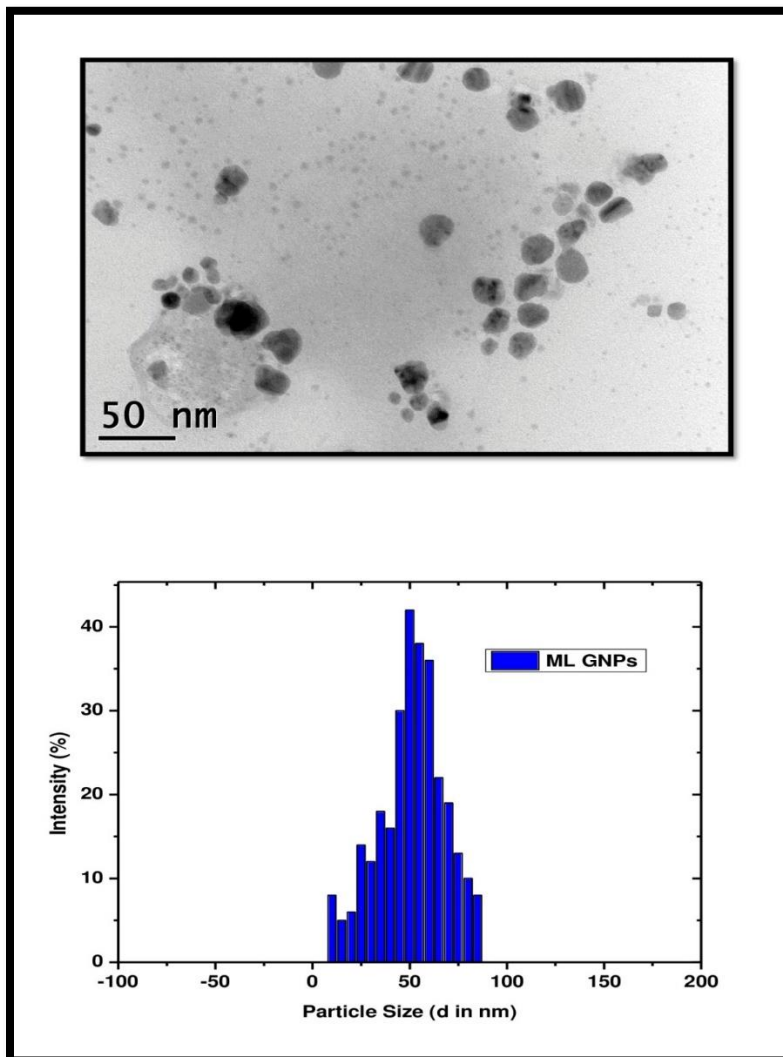


Fig. 2. HR-TEM image and particles size analysis (PSA) of ML-GNPs

The FTIR spectra of the samples were analyzed to determine the hydrocarbon groups of the extract in the synthesized GNPs. The FTIR spectra of the stabilized GNPs revealed an interface amongst the GNPs besides extract. The broad absorbance found at 3000 to 3300 cm^{-1} is indicative of strong H-bonding, along with N-H, O-H stretching vibration (Park *et al.* 2007; Mohammad and Hamid 2011; Hamley *et al.* 2013; Ismail *et al.* 2013). A weak band appeared at roughly 2930 cm^{-1} , which may relate to aliphatic group C-H vibration. The solid immersion range at 1639.3 cm^{-1} was identified as the amide-I group, which was primarily demonstrative of C=O elongating vibrations (Chimentão *et al.* 2006; Malhotra *et al.* 2013; Manivasagan *et al.* 2015; Yallappa *et al.* 2016; Dhayalan *et al.* 2018). In terms of the band criterion, the strong broad band at 3400 cm^{-1} is related to NH stretching of biological compounds, the broadening of which results from inter/intramolecular H-bonding. A weak band appearing at roughly 2930 cm^{-1} may correspond to the C-H stretching of hydrocarbons. The peak at 1660 cm^{-1} and the weaker band at 1450 cm^{-1} were attributed to the asymmetric and symmetric stretching of hydroxyl (single-bonded OH), in that order. The spectra signs equivalent to the stretching vibration of the $\text{-SO}_3\text{H}$ and C-O-S groups produced spectral signals at approximately 1260, 1086, and 850 cm^{-1} .

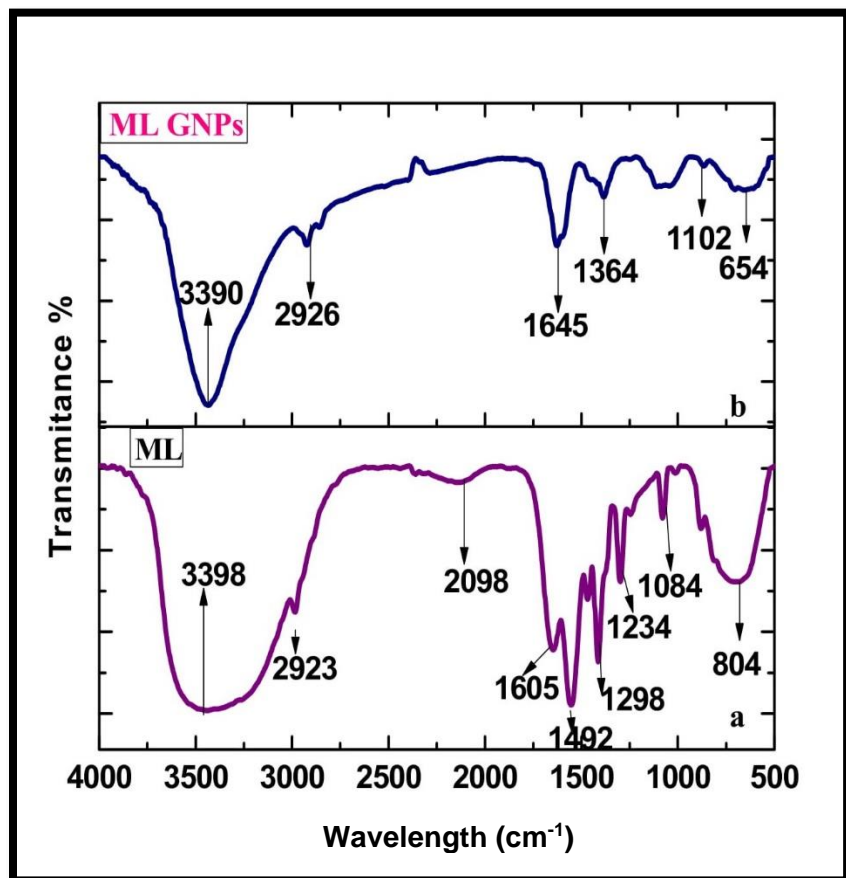


Fig. 3. FTIR spectra from ML–GNPs and *Madhuca longifolia* seed extract (ML)

X-ray Diffraction Studies

The prepared GNPs were also analyzed by XRD, and the pattern is shown in Fig. 4. Four strong bands were detected in the XRD pattern that matched GNPs and had intensities between 10 and 80. These peaks exhibited Bragg-reflection-like patterns (Nakkala *et al.* 2016; Dhayalan *et al.* 2017). These findings are consistent with previous research (Nguyen *et al.* 2019). The XRD spectra with prominent characteristic peaks observed at $2\theta = 39.1, 44.3, 64.50,$ and 77.70° , were consistent with the Bragg reflections (111), (200), (220), and (311) planes of Au crystals. These correspondingly, were indexed to face centers cubic lattice structure of GNPs (Pragathiswaran *et al.* 2020; JCPDS.NO.04-0784). The average crystallite size of samples was calculated by using Debye–Scherrer’s formula,

$$D = \frac{(0.89 \times \lambda)}{(\beta \cos \theta)} \quad (1)$$

where D is the average crystallite size, λ is the X-ray wavelength, θ is the Bragg diffraction angle, and β is the full width at half maximum (FWHM). The average crystallite size was found to be 24.98 nm

Biological Application

Antioxidant assay

The antioxidant activity of *M. longifolia* seed extract and GNPs was investigated using DPPH and phosphomolybdenum assays at several concentrations (20, 40, 60, 80, and 100 $\mu\text{g/mL}$) (Fig. 5). Through deriving electrons or hydrogen atoms from GNPs, free radical molecules in DPPH are decolorized, and are measured spectrophotometrically. The proportion reticence of chain breaking during antioxidant activity is shown in Fig. 5. Aggregated GNPs inhibit free radicals in a dosage-dependent manner. The fraction of reticence increased with cumulative concentrations of *M. longifolia* extract. The GNPs Antioxidant activity was greater than the control and it increased with increasing concentrations of *M. longifolia* extract and GNPs (Iyabo *et al.* 2017). Maximum concentration (100 $\mu\text{g/mL}$), maximum DPPH scavenging activities of extract, and GNPs are shown in Fig. 5.

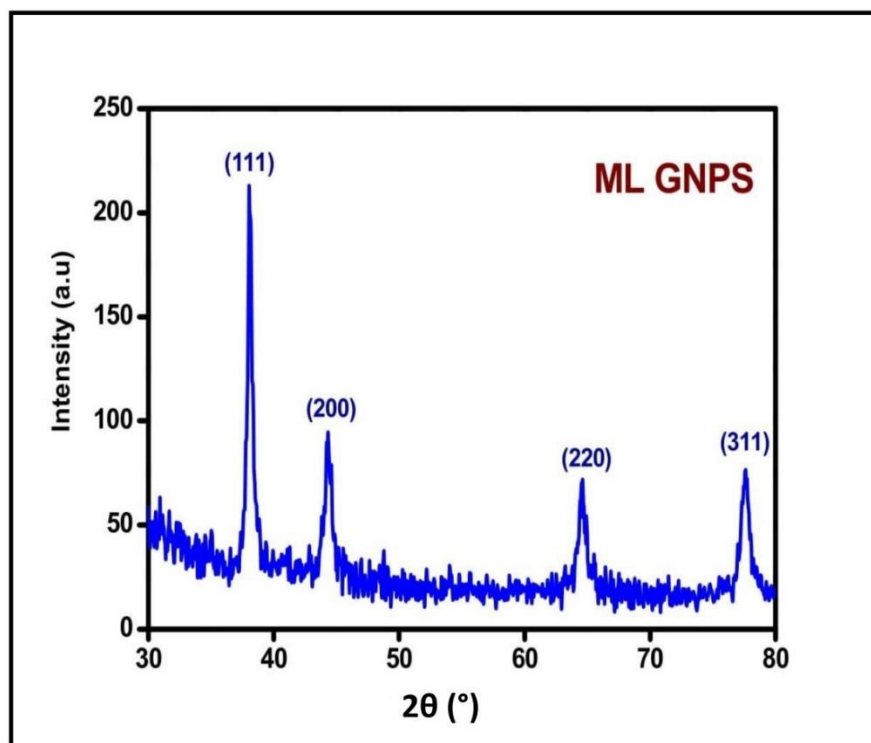


Fig. 4. XRD peaks for ML-GNPs

Numerous studies have demonstrated that the extract has more antioxidant activity than synthetic GNPs, which is consistent with the current findings (Geethalakshmi and Sarada 2012). The phosphomolybdenum assay has been able to define the capability to extricate to decrease Mo(VI) to Mo(V) and then form a $\text{CrPO}_4 \cdot (\text{H}_2\text{O})_n / \text{Mo(V)}$ composite at an acidic pH. Similar outcomes were obtained in the phosphomolybdenum assay, such as increased activity of antioxidant along with increasing concentrations of the *M. longifolia* and GNPs.

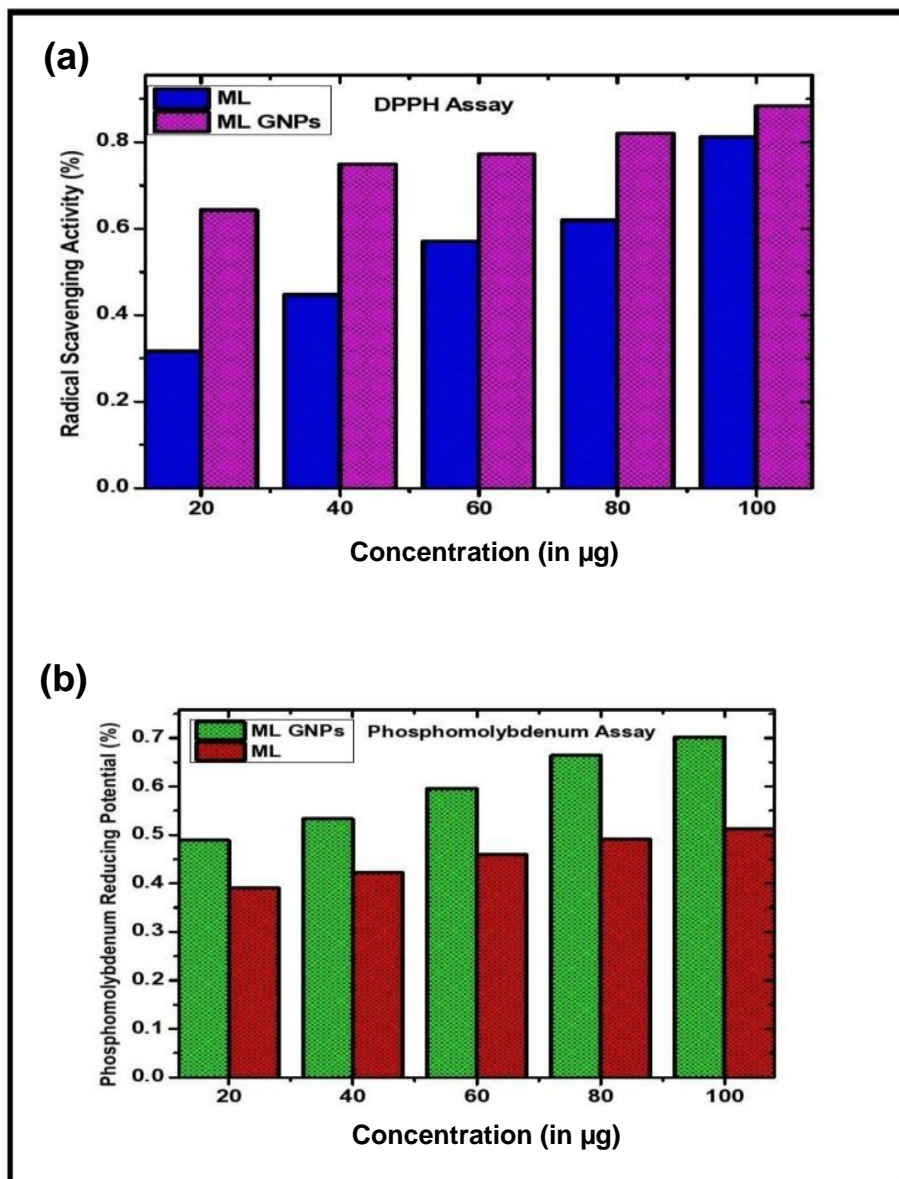


Fig. 5. (a) DPPH radical scavenging activity of ML-GNPs with (ML) control; (b) phosphomolybdenum reducing potential of ML-GNPs (ML) control

MTT Assay

The GNPs were tested for cytotoxicity against the A549 cancer cell line. Figure 6 shows how synthetic GNPs were built on the A549 cell line and then monitored for cell viability using the MTT assay. Compared with untreated cells, cells treated with GNPs had a lower rate of metabolism (control). The dosage of nanoparticles affected cell viability. The GNP concentrations (1, 10, 100, 1, 10, and 100 µg/mL) remarkably reduced cell viability. The IC₅₀ values of the ML-GNPs were at 29.5 µg/mL. Figure 6 depicts the viability of cancer cells after 24 and 48 h of treatment.

Antibacterial activity

The effects of the antiseptic susceptibility test for different concentrations of ML-GNPs against *Micrococcus luteus* and *Proteus vulgaris* are shown in Fig. 7. The results showed that ML-GNPs were most effective against *Micrococcus luteus*. This demonstrated the uppermost activity against *Micrococcus luteus*, with a zone of inhibition 3 to 13 mm per 100 g/mL, tracked by the maximum action against *Proteus vulgaris*, with a zone of inhibition 11 to 17 mm per 100 g/mL.

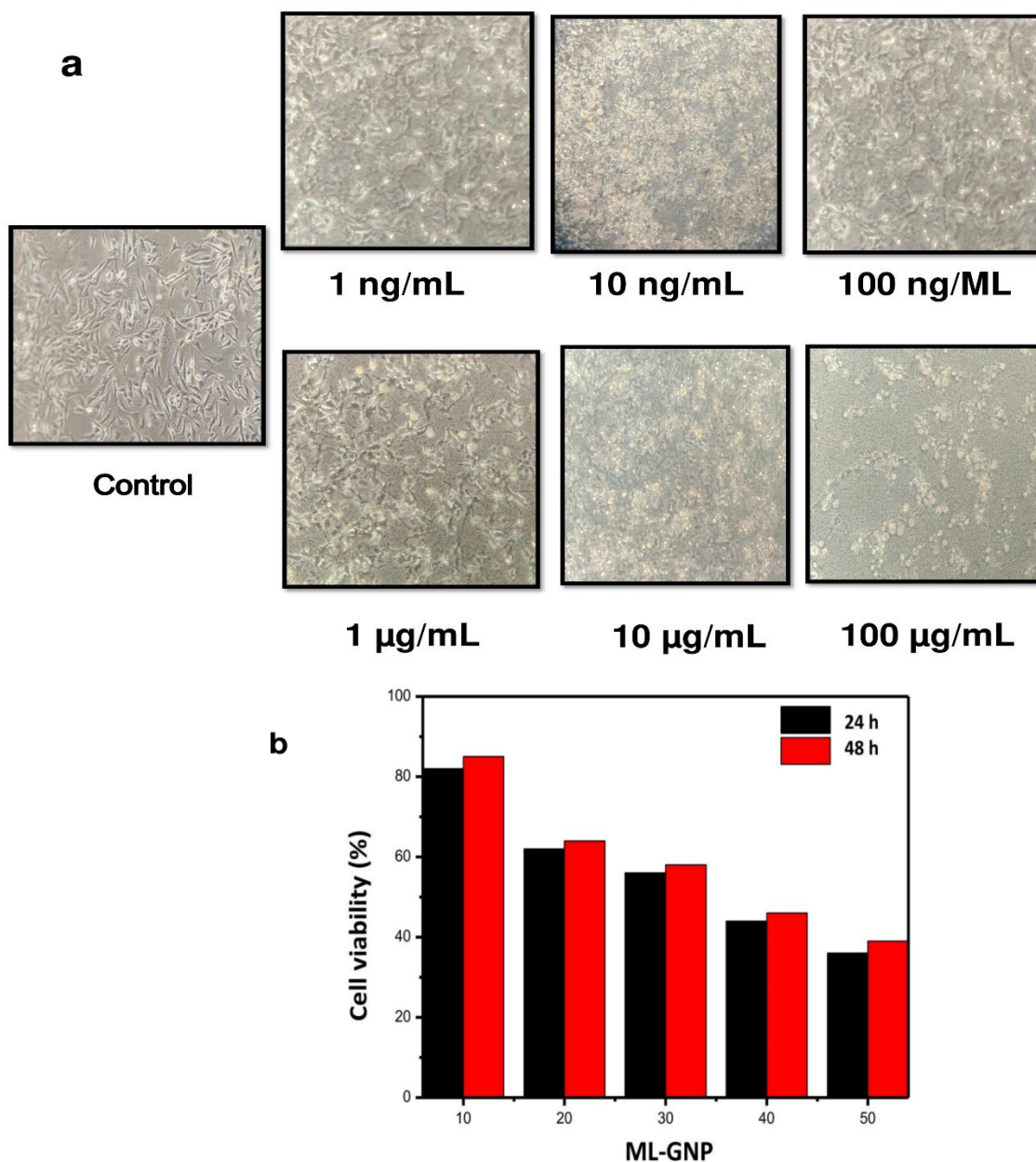


Fig. 6.a & b. MTT assay for cell viability at different concentrations (1 ng/mL, 10 ng/mL, 100 ng/mL, 1 µg/mL, 10 µg/mL, and 100 µg/mL) of ML-GNPs dignified by MTT assay on A549 cell line

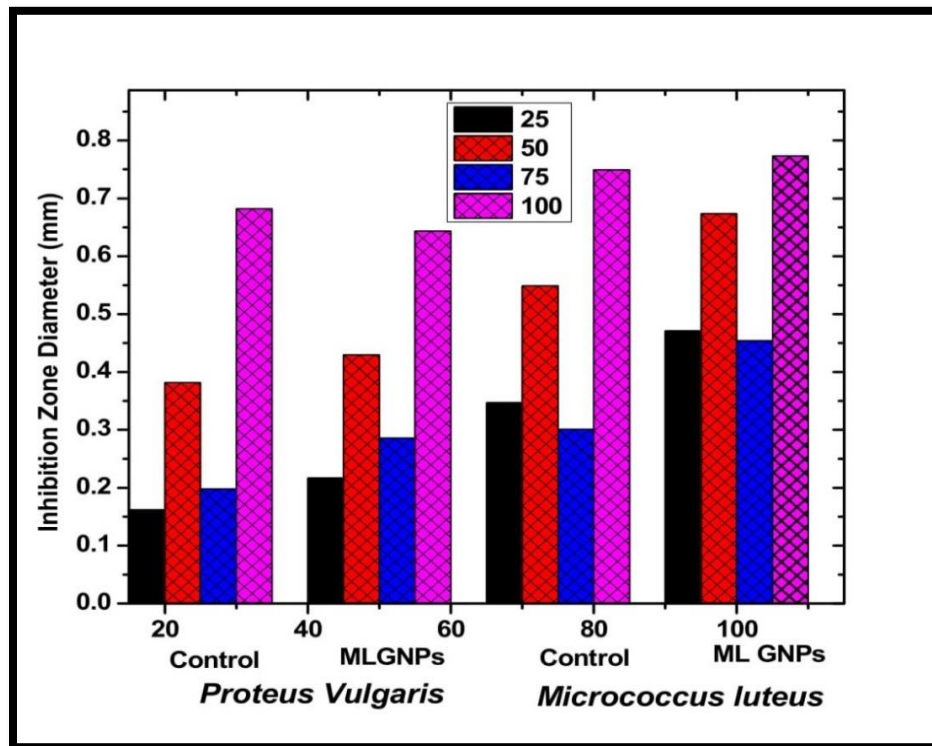


Fig. 7. Antibacterial activity of ML-GNPs in contradiction of *Proteus vulgaris* and *Micrococcus luteus*

Possible antimicrobial mechanisms of MNPs include the release of toxic ions and damaging modifications to proton efflux bombs and cell walls. These processes are caused by the breakdown of intracellular proteins, DNA, RNA, and cell walls.

Minimal inhibitory concentration (MIC)

An MIC assay was carried out to determine the minimum inhibitory attentiveness of biogenic GNPs in contradiction of bacteriological strains. The MIC examination was used to determine whether antibacterial activity was present at different dosage levels. The MIC examination rate of biogenic GNPs in contradiction of both strains of *Proteus vulgaris* MTCC No:742, NCTC8311, and *Micrococcus luteus* MTCC No:1538 were calculated as 0.29 and 0.96 mg/mL, respectively, and that of triclosan was considered as 0.4 and 2 mg/mL, in this current study (Fig. 8). It is worth mentioning that the IC₅₀ value was substantially lower than the IC₅₀ value of commercially available medicines. The GNPs synthesized from several plant extracts have been found effective against various bacteria. Geethalakshmi and Sarada (2012) found that Ag and GNPs synthesized from *Coleus forskohlii* had outstanding activity against, *Proteus vulgaris*, *E. coli*, and *S. aureus*, with zones of inhibition at 12.5 to 14.5 mm for GNPs and 14.5 to 21.6 mm for nanoparticles. The biochemical, optical, and thermal properties of metal nanoparticles are influenced by their size and shape, which in turn is important for their antimicrobial activity (Chandrasekaran *et al.* 2022).

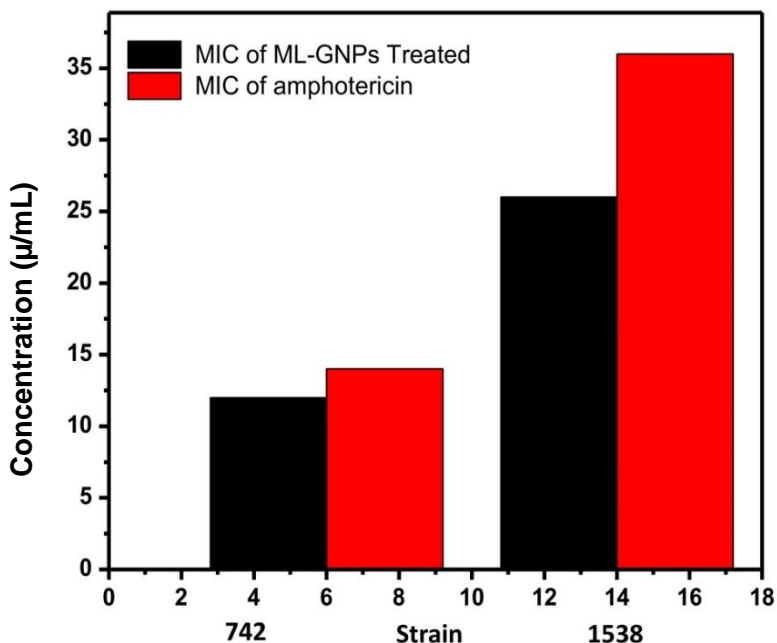


Fig. 8. MIC of ML-GNP towards the bacterial strains

Phytoconstituents in seed extract of Madhuca longifolia

Phytoconstituents analysis for ML extract indicated the presence of various phytoconstituents, such as flavonoids, carbohydrates, saponins, strains, glycosides, proteins, alkaloids, and amino acids, all of which are responsible for various pharmacological actions, implying that further research is needed to investigate their potential as healing techniques.

CONCLUSIONS

In this study, gold nanoparticles (ML-GNPs) derived successfully from *Madhuca longifolia* seed aqueous extract were used as a simple, cost-effective, eco-friendly, and rapid green synthesis method. They were evaluated by various physicochemical characterizations and analytical techniques. The examination exemplified in this report was the cytotoxic activity against adherent human lung carcinoma A549 cells using the MTT assay, and the observed IC_{50} values were $\sim 29.5 \mu\text{g}/\text{mL}$. Therefore, such nanoparticles may be used as an anti-carcinogenic agent. Furthermore, from a relative study of antioxidant properties against DPPH and phosphomolybdenum assays, the bacterial strains *Proteus vulgaris* and *Micrococcus luteus* showed that ML-GNPs can be used to formulate nanomedicines after successive established investigations. The results of this study can be helpful to develop the examination of the therapeutics prospective of ML-GNPs in the future.

DECLARATIONS

Ethics Approval and Consent to Participate

All authors have approved and have consent.

Availability of Data and Materials

Data will be available as and when required.

Competing Interests

The authors have declared that no competing interests exist.

ACKNOWLEDGMENTS

The authors acknowledge the funding from Researchers Supporting Project number (RSP2023R54), King Saud University, Riyadh, Saudi Arabia.

The authors acknowledge the Animal Tissue culture Unit, PG & Research Department of Biotechnology, Islamiah College (Autonomous), Vaniyambadi – 635752 for cell culture studies.

REFERENCES CITED

- Abdoli, M., Arkan, E., Shekarbeygi, Z., and Khaledian, S. (2021). “Green synthesis of gold nanoparticles using *Centaurea behen* leaf aqueous extract and investigating their antioxidant and cytotoxic effects on acute leukemia cancer cell line (THP-1),” *Inorganic Chemistry Communications* 129, article ID 108649. DOI: 10.1016/j.inoche.2021.108649
- Ahati, P., Xu, T., Chen, L., and Fang, H. (2022). “Biosynthesis, characterization and evaluation of anti-bone carcinoma, cytotoxicity, and antioxidant properties of gold nanoparticles mediated by *Citrus reticulata* seed aqueous extract: Introducing a novel chemotherapeutic drug,” *Inorganic Chemistry Communications* 143, article ID 109791. DOI: 10.1016/j.inoche.2022.109791
- Chandrasekaran, S., Anusuya, S., and Anbazhagan, V. (2022). “Anticancer, anti-diabetic, antimicrobial activity of zinc oxide nanoparticles: A comparative analysis,” *Journal of Molecular Structure* 1263, article 133139. DOI: 10.1016/j.molstruc.2022.133139.
- Chimentão, R. J., Cota, I., Dafinov, A., Medina, F., Sueiras, J. E., Gómez de la Fuente, J. L., Fierro, J. L. G., Cesteros, Y., and Salagre, P. (2006). “Synthesis of silver-gold alloy nanoparticles by a phase-transfer system,” *Journal of Materials Research* 21, 105-111. DOI: 10.1557/jmr.2006.0014
- Chinky, G., Bushra, Y., Rashmi, N., Abu, B., Naushin, B., Narendra, K., and Radhey, M. (2023). “*Madhuca longifolia* leaves mediated palladium nanoparticles synthesis via a sustainable approach to evaluate its biomedical application,” *Chemical Papers* 77, 3075-3091. DOI: 10.1007/s11696-023-02688-5
- Darroudi, M., Ahmad, M. B., Hakimi, M., Zamiri, R., Khorsand Zak, A., Hosseini, H. A., and Zargar, M. (2013). “Preparation, characterization and antibacterial activity of -irradiated silver nanoparticles in aqueous gelatin,” *International Journal of Minerals, Metallurgy, and Materials* 20, 403-409. DOI: 10.1007/s12613-013-0743-2

- Darroudi, M., Ahmad, M. B., Zak, A. K., Zamiri, R., and Hakimi, M. (2011a). "Fabrication and characterization of gelatin stabilized silver nanoparticles under UV-light," *International Journal of Molecular Sciences* 12(9), 6346-6356. DOI: 10.3390/ijms12096346
- Darroudi, M., Ahmad, M. B., Zamiri, R., Abdullah, A. H., Ibrahim, N. A., and Sadrolhosseini A. R. (2011b). "Time-dependent preparation of gelatin-stabilized silver nanoparticles by pulsed Nd: YAG laser," *Solid State Sciences* 13(3), 520-524. DOI: 10.1016/j.solidstatesciences.2010.12.018
- Darroudi, M., Ahmad, M. B., Zamiri, R., Abdullah, A. H., Ibrahim, N. A., Shameli, K., and Husin, M. S. (2011c). "Preparation and characterization of gelatin mediated silver nanoparticles by laser ablation," *Journal of Alloys and Compounds* 509(4), 1301-1304. DOI: 10.1016/j.jallcom.2010.10.018
- Darroudi, M., Khorsand Zak, A., Muhamad, M. R., Huang, N. M., and Hakimi, M. (2012). "Green synthesis of colloidal silver nanoparticles by sonochemical method," *Materials Letters* 66(1), 117-120. DOI: 10.1016/j.matlet.2011.08.016
- Dhayalan, M., Jesse Denison, M. I., Jegadeeshwari, A., Krishnan, K., and Nagendra Gandhi, N. (2017). "In vitro antioxidant, antimicrobial, cytotoxic potential of gold and silver nanoparticles prepared using *Embelia ribes*," *Natural Product Research* 31(4), 465-468. DOI: 10.1080/14786419.2016.1166499
- Dhayalan, M., Jesse Denison, M. I., Manikandan, A., Nagendra Gandhi, N., Krishnan K., and Baykal, A. (2018). "Biogenic synthesis, characterization of gold and silver nanoparticles from *Coleus forskohlii* and their clinical importance," *Journal of Photochemistry and Photobiology B: Biology* 183, 251-257. DOI: 10.1016/j.jphotobiol.2018.04.042
- Dhayalan, M., Malathi, S., Karthick, K. B., Mohammed Riyaz, S. U., and Mika, S. (2021). "Eco friendly synthesis and characterization of zinc oxide nanoparticles from *Aegle marmelos* and its cytotoxicity effects on MCF-7 cell lines," *Nanofabrication* 6, 44-51. DOI: 10.1515/nanofab-2020-0104
- Elia, P., Zach, R., Hazan, S., Kolusheva, S., Porat, Z., and Zeiri, Y. (2014). "Green synthesis of gold nanoparticles using plant extracts as reducing agents," *International Journal of Nanomedicine* 9, article 4007. DOI: 10.2147/IJN.S57343
- Faramarzi, M. A., and Farootanfar, H. (2011). "Biosynthesis and characterization of gold nanoparticles produced by laccase from *Paraconiothyrium variable*," *Colloids and Surfaces B: Biointerfaces* 87(1), 23-27. DOI: 10.1016/j.colsurfb.2011.04.022
- Geethalakshmi, R., and Sarada, D. V. L. (2012). "Gold and silver nanoparticles from *Trianthema decandra*: Synthesis, characterization, and antimicrobial properties" *International Journal of Nanomedicine* 7, 5375–5384. DOI: 10.2147/IJN.S36516
- Hamley, I. W., Dehsorkhi, A., Jauregi, P., Seitsonen, J., Ruokolainen, J., Coutte, F., Chataigné, G., and Jacques, P. (2013). "Self-assembly of three bacterially-derived bioactive lipopeptides," *Soft Matter* 9, 9572-9578. DOI: 10.1039/C3SM51514A
- Homa, H., Pradakshina, S., Mohd, R. H., Shiwani, S., Deepanshi, T., and Jagriti, N. (2022). "Gold nanomaterials – The golden approach from synthesis to applications," *Materials Science for Energy Technologies* 5, 375-390. DOI: 10.1016/j.mset.2022.09.004
- Hosny, M., Eltaweil, A. S., Mostafa, M., El-Badry, Y.A., Hussein, E. E., Omer, A. M., and Fawzy, M. (2022). "Facile synthesis of gold nanoparticles for anticancer, antioxidant applications, and photocatalytic degradation of toxic organic pollutants," *ACS Omega* 7, 3121-3133, DOI: 10.1021/acsomega.1c06714

- Iyabo, C. I., Agbaje, L., Joseph, A. E., Musibau, A. A., Tesleem, B. A., Taofeek, A. Y., Akeem, A., Evariste, B. G.-K., Lorika, S. B., Tolulope, O. O., *et al.* (2017). “*Enterococcus* species for the one-pot biofabrication of gold nanoparticles: Characterization and nanobiotechnological applications,” *Journal of Photochemistry and Photobiology B: Biology* 173, 250-257. DOI: 10.1016/j.jphotobiol.2017.06.003
- Jayashree, S., Dhayalan, M., Mohammed Riyaz, S. U., Mayakkannan, G., Ali Khan, M., Simal-Gandara, J., and Cid-Samamed, A. (2022). “Green synthesis of silver nanoparticles using *Allium cepa* var. *aggregatum* natural extract: Antibacterial and cytotoxic properties nanomaterials,” *Nanomaterials* 12(10), article 1725. DOI: 10.3390/nano12101725
- Kahrilas, G. A., Haggren, W., Read, R. L., Wally, L. M., Fredrick, S. J., Hiskey, M., Prieto, A. L., and Owens, J. E. (2014). “Investigation of antibacterial activity by silver nanoparticles pre-pared by microwave- assisted green syntheses with soluble starch, dextrose and arabinose,” *ACS Sustainable Chemistry & Engineering* 2(4), 590-598. DOI: 10.1021/sc400487x
- Khan, A. K., Rashid, R., Murtaza, G., and Zahra, A. (2014). “Gold nanoparticles: Synthesis and applications in drug delivery,” *Tropical Journal of Pharmaceutical Research* 13(7), 1169-1177. DOI: 10.4314/tjpr.v13i7.23
- Kucherenko, I. S., Soldatkin, O. O., Kucherenko, D. Y., Soldatkina, O. V., and Dzyadevych, S. V. (2019). “Advances in nanomaterial application in enzyme-based electrochemical biosensors: A review,” *Nanoscale Advances* 1(12), 4560-4577. DOI: 10.1039/C9NA00491B
- Kutsenko, A. S., and Granchak, V. M. (2009). “Photochemical synthesis of silver nanoparticles in polyvinyl alcohol matrices,” *Theoretical and Experimental Chemistry* 45, 313-318. DOI: 10.1007/s11237-009-9099-0
- Malhotra, A., Dolma, K., Kaur, N., Rathore, Y. S., Mayilraj, S., and Choudhury, A. R. (2013). “Biosynthesis of gold and silver nanoparticles using a novel marine strain of *Stenotrophomonas*,” *Bioresource Technology* 142, 727-731. DOI: 10.1016/j.biortech.2013.05.109
- Manivasagan, P., Alam, M. S., Kang, K., Kwak, M., and Kim, S. (2015). “Extracellular synthesis of gold bionanoparticles by *Nocardioopsis* sp. and evaluation of its antimicrobial, antioxidant and cytotoxic activities,” *Bioprocess and Biosystems Engineering* 38, 1167-1177. DOI: 10.1007/s00449-015-1358-y
- Mohammad, A. F., and Hamid, F. (2011). “Biosynthesis and characterization of gold nanoparticles produced by laccase from *Paraconiothyrium variabile*,” *Colloids and Surfaces B: Biointerfaces* 87(1) 23-27. DOI: 10.1016/j.colsurfb.2011.04.022
- Nakkala, J. R., Mata, R., and Sadras, S. R. (2016). “The antioxidant and catalytic activities of green synthesized gold nanoparticles from *Piper longum* fruit extract,” *Process Safety and Environmental Protection* 100, 288-294. DOI: 10.1016/j.psep.2016.02.007
- Nguyen, V. T., Vu, V. T., Nguyen, T. A., Tran, V. K., and Nguyen-Tri, P. (2019). “Antibacterial activity of TiO₂- and ZnO- decorated with silver nanoparticles,” *Journal of Composites Science* 3(2), article 61. DOI: 10.3390/jcs3020061
- Ohadi, M., Dehghannoudeh, G., Forootanfar, H., Shakibaie, M., and Rajaei, M. (2018). “Investigation of the structural, physicochemical properties and aggregation behavior of lipopeptide biosurfactant produced by *Acinetobacter junii* B6,” *International Journal of Biological Macromolecules* 112, 712-719. DOI: 10.1016/j.ijbiomac.2018.01.209

- Panda, T., and Deepa, K. (2011). "Biosynthesis of gold nanoparticles," *Journal of Nanoscience and Nanotechnology* 11(12), 10279-10294. DOI: 10.1166/jnn.2011.5021
- Pandey, P. K., Gangwar, C., Yaseen, B., Kumar, I., Nayak, R., Kumar, S., Naik, R. M., Banerjee, M., and Sarker, J. (2023). "Anticancerous and antioxidant properties of fabricated silver nanoparticles involving bio organic framework using medicinal plant *Blumea lacera*," *Chemical Papers* 77, 3603-3617. DOI:10.1007/s11696-023-02723-5
- Park, J., Joo, J., Kwon, S. G., Jang, Y., and Hyeon, T. (2007). "Synthesis of monodisperse spherical nanocrystals," *Angewandte Chemie- International Edition* 46(25), 4630-4660. DOI: 10.1002/anie.200603148
- Patil, M. P., and Kim, G. D. (2017). "Eco-friendly approach for nanoparticles synthesis and mechanism behind antibacterial activity of silver and anticancer activity of gold nanoparticles," *Applied Microbiology and Biotechnology* 101(1), 79-92. DOI: 10.1007/s00253-016-8012-8
- Patil, M. P., Bayaraa, E., Subedi, P., Piad, L. L. A., Tarte, N. H., and Kim, G.-D. (2019). "Biogenic synthesis, characterization of gold nanoparticles using *Lonicera japonica* and their anticancer activity on HeLa cells," *Journal of Drug Delivery Science and Technology* 51, 83-90. DOI: 10.1016/j.jddst.2019.02.021
- Patil, M. P., Jin, X., Simeon, N. C., Palma, J., Kim, D., Ngabire, D., Kim, N.-H., Tarte, N. H., and Kim, G.-D. (2018). "Anticancer activity of *Sasa borealis* leaf extract-mediated gold nanoparticles," *Artificial Cells, Nanomedicine, and Biotechnology* 46(1), 82-88. DOI: 10.1080/21691401.2017.1293675
- Patil, M. P., Ngabire, D., Thi, H. H. P., Kim M.-D., and Kim, G.-D. (2017). "Eco-friendly synthesis of gold nanoparticles and evaluation of their cytotoxic activity on cancer cells," *Journal of Cluster Science* 28, 119-132. DOI: 10.1007/s10876-016-1051-6
- Pragathiswaran, C., Smith, C., Barabadic, H., Al-Ansari, M. M., Al-Humaid, L. A., and Saravanan, M. (2020). "TiO₂@ZnO nanocomposites decorated with gold nanoparticles: Synthesis, characterization and their antifungal, antibacterial, anti-inflammatory and anticancer activities," *Inorganic Chemistry Communications* 121, article ID 108210. DOI: 10.1016/j.inoche.2020.108210
- Roat, P., Hada, S., Chechani, B., Kumar Yadav, D., Kumar, S., and Kumari, N. (2023). "*Madhuca indica*: A review on the phytochemical and pharmacological aspects," *Pharm. Chem. J.* 57, 284-295. DOI: 10.1007/s11094-023-02878-1
- Sengani, M., Grumezescu, A. M., and Rajeswari, V. D. (2017). "Recent trends and methodologies in gold nanoparticle synthesis – A prospective review on drug delivery aspect," *OpenNano* 2, 37-46. DOI: 10.1016/j.onano.2017.07.001
- Shameli, K., Ahmad, M. B., Yunus, W. Z. W., Ibrahim, N. A., and Darroudi, M. (2010). "Synthesis and characterization of silver/talc nanocomposites using the wet chemical reduction," *International Journal of Nanomedicine* 5, 743-751. DOI: 10.2147/IJN.S13227
- Singh, B. R., Dwivedi, S., Al-Khedhairi, A. A., and Musarrat, J. (2011). "Synthesis of stable cadmium sulfide nanoparticles using surfactin produced by *Bacillus amyloliquifaciens* strain KSU-109," *Colloids and Surfaces B: Biointerfaces* 85(2), 207-213. DOI: 10.1016/j.colsurfb.2011.02.030
- Smitha, S. L., Philip, D., and Gopchandran, K. G. (2009). "Green synthesis of gold nanoparticles using *Cinnamomum zeylanicum* leaf broth," *Spectrochimica Acta Part A: Molecular and Biomolecular Spectroscopy*. 74(3), 735-739. DOI: 10.1016/j.saa.2009.08.007

- Tahir, M. Y., Sillanpaa, M., Almutairi, T. M., Mohammed, A. A. A., and Ali, S. (2023). "Excellent photocatalytic and antibacterial activities of bio-activated carbon decorated magnesium oxide nanoparticles," *Chemosphere* 312(Part 2), article ID 137327. DOI: 10.1016/j.chemosphere.2022.137327
- Yallappa, S., Manjanna, J., Dhananjaya, B. L., Vishwanatha, U., Ravishankar, B., Gururaj, H., Niranjana, P., and Hungund, B. S. (2016). "Phytochemically functionalized Cu and Ag nanoparticles embedded in MWCNTs for enhanced antimicrobial and anticancer properties," *Nanomicro Letters* 8(2), 120-130. DOI: 10.1007/s40820-015-0066-0
- Yang, Y., Sun, H., Awwad, N. S., Ibrahim, H. A., Alhomaid, F. A., El-Kott, A. F., and Abdel-Daim, M. M. (2022). "Gold nanoparticles immobilized over kaolin-modified mentha extract: Investigation of its antioxidant and anticancer effects against cervical adenocarcinoma cancer cells as a novel chemotherapy agent," *Inorganic Chemistry Communications* 138, article ID 109125. DOI: 10.1016/j.inoche.2021.109125
- Yin, B., Ma, H., Wang, S., and Chen, S. (2003). "Electrochemical synthesis of silver nanoparticles under protection of poly(N-vinylpyrrolidone)," *The Journal of Physical Chemistry B* 107(34), 8898-8904. DOI: 10.1021/jp0349031

Article submitted: September 22, 2023; Peer review completed: November 26, 2023;
Revised version received and accepted: December 4, 2023; Published: December 11, 2023.

DOI: 10.15376/biores.19.1.823-841